Transient State Analysis of Porcine Dihydropyrimidine Dehydrogenase Reveals Reductive Activation by NADPH.

Brett A. Beaupre, Dariush C. Forouzesh and Graham R. Moran*

Department of Chemistry and Biochemistry, 1068 W Sheridan Rd, Loyola University Chicago, Chicago, IL 60660

^{*}corresponding author; phone: (773)508-3756; email: gmoran3@luc.edu

Abstract

Dihydropyrimidine dehydrogenase (DPD) catalyzes the initial step in the catabolism of the pyrimidines uracil and thymine. Crystal structures have revealed an elaborate subunit architecture consisting of two flavin cofactors, apparently linked by four Fe₄S₄ centers. Analysis of the DPD reaction(s) equilibrium position under anaerobic conditions revealed a reaction that favors dihydropyrimidine formation. Single-turnover analysis shows biphasic kinetics. The serine variant of the candidate general acid, cysteine 671, provided enhanced kinetic resolution for these phases. In the first event, one subunit of the DPD dimer takes up two electrons from NADPH in a reductive activation step. Spectrophotometric deconvolution suggests that thes electrons reside on one of the two flavins. That oxidation of the enzyme by dioxygen can be suppressed by the addition of pyrimidine, is consistent with these electrons residing on the FMN. The second phase involves further oxidation of NADPH and concomitant reduction of the pyrimidine substrate. During this phase no net reduction of DPD cofactors is observed indicating that the entire cofactor set acts as a wire, transmitting electrons from NADPH to the pyrimidine rapidly. This indicates that the availability of the proton from C671 general acid controls the transmittance of electrons from NADPH to the pyrimidine. Acid quench and HPLC product analysis of single-turnover reactions with limiting NADPH confirmed 2:1, NADPH:pyrimidine stoichiometry for the enzyme accounting for successive activation and pyrimidine reduction. These data support an alternating subunit model in which one protomer is activated and turns over before the other subunit can be activated and enter catalysis.

Introduction

Uracil and thymine bases are the oxidant substrates for dihydropyrimidine dehydrogenase (DPD). DPD reduces the pyrimidine 5,6-vinylic bond with electrons derived from NADPH (Scheme 1).

Scheme 1: The chemistry catalyzed by DPD

This reaction is reversible and reported to be the rate-limiting step in the catabolism of pyrimidines to aminoisobutyrate (thymine) or beta-alanine (uracil)^{1.5}. In addition to native pyrimidines, DPD will reduce a variety of 5-substituted uracils ^{1, 6, 7} including one of the most commonly prescribed cytotoxic agents used in the treatment of cancer, 5-fluorouracil (5FU). 5FU was offered as a potential tumor cell toxicant in the late 1950s in response to the discovery that rat liver tumor cells sequestered uracil at a higher rate than normal cells⁸⁻¹¹. Nearly isosteric with uracil, 5FU is incorporated into both RNA and DNA where it disrupts post-transcriptional modifications and interferes with replication^{11, 12}. However, its primary mode of action is via 5FdUMP, a potent inhibitor of thymidylate synthase (TS)^{13, 14}. Inhibition of TS hinders DNA synthesis and repair dictating that 5FU toxicity is heightened for cells undergoing rapid growth and division¹⁵. The pharmacokinetic rate of 5FU detoxification by DPD is rapid with a half-life of ~ 20 minutes^{16, 17}. DPD therefore undermines the antineoplastic potential of 5FU and is a central mitigating factor in the treatment of numerous cancers^{15, 18}. Modulation of DPD activity by inhibition therefore has stood as a promising path to enhanced fluoropyrimidine efficacy^{15, 17-22}.

Despite the importance of DPD with regard to the efficacy potential of 5FU, relatively little definitive data has been published that accounts for its catalytic behavior or inhibition, a point noted by Schnackerz et al. in the most recent review available²³. In nature the type of chemistry catalyzed by DPD is more often catalyzed by a flavoprotein that has a single ligand binding cavity and exhibits what is known as a ping-pong kinetic mechanism. In such a mechanism the enzyme initially binds NAD(P)H and accepts a hydride. Upon the release of NAD(P)+ the enzyme then acquires and reduces an oxidant substrate²⁴⁻²⁶. DPD accomplishes each of these steps but utilizes two ligand binding sites ~56 Å apart that each have a flavin cofactor.

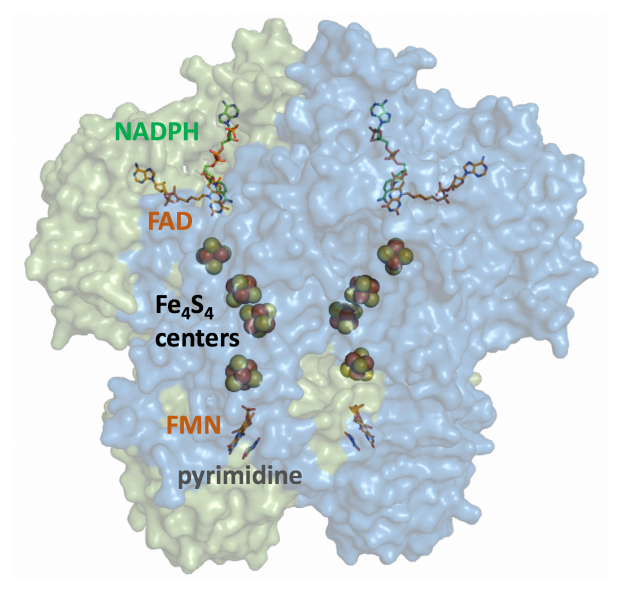
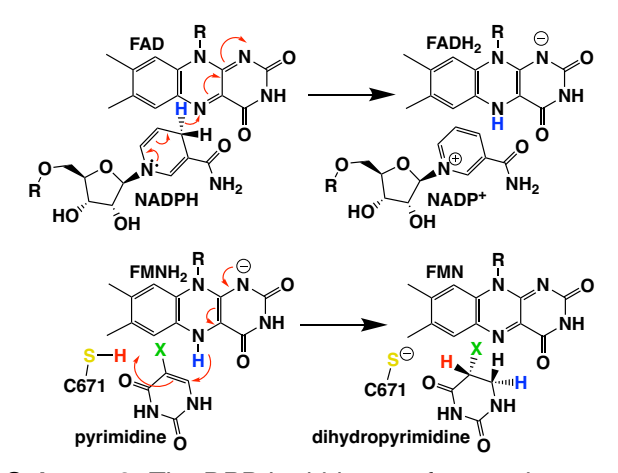


Figure 1. The structure of the DPD dimer (PDB ID : 1H7X)

The flavins of DPD are connected by an apparent wire composed of four Fe₄S₄ centers^{7, 27}. The quaternary structure is a head-to-head homodimer with a large buried interface of ~10,800 Å². Each subunit has an FAD site that binds NADPH and an FMN site that binds pyrimidine bases (Figure 1). The enzyme is a functional dimer; each protomer has four Fe₄S₄ centers but each provides two of the four centers that complete the conduit in the other subunit²⁷. Given the simplicity of the chemistry catalyzed, the DPD architecture is seemingly unnecessarily elaborate.

Nonetheless, the enzyme's structure does not by itself indicate that the mechanism at work is anything more complex than a linear transfer of electrons from NADPH to the pyrimidine base. What is not apparent from the structure or in any published work is where electrons reside at intervening stages of catalysis.

Much of the biochemical data published for DPD describes purification and rudimentary characterization of various homologs^{1, 4, 5, 28, 29}. Two structural studies of the enzyme have been published both of which include structures of ternary complexes with NADPH and a form of pyrimidine bound^{7, 27}. These ternary complex structures (PDB IDs: 1H7X, 1GT8 & 1GTH) have the ligands positioned appropriately for hydride transfer to and from the N5 of the flavins and so provide a clear understanding of the active site interactions. This has led directly to a hypothetical chemical mechanism (Scheme 2)³⁰.



Scheme 2: The DPD hydride transfer reactions

Under steady-state conditions, specific forms of DPD produce parallel lines in Lineweaver-Burk plots with respect to both substrates; traditionally interpreted as ping-pong kinetics ^{5, 29}. For DPD, such a mechanism suggests an intervening reduced state of the enzyme. However, bacterial

and bovine DPD exhibited steady-state kinetic patterns consistent with a rapid equilibrium random mechanism that predicts both substrates are bound prior to the chemistry^{4, 31}. These apparent homolog-dependent kinetic mechanism differences are, from a chemical mechanism standpoint, not mutually exclusive and likely reflect different ligand-gated contingencies for electron transfer between the active sites. However, it is of note that by themselves, these designations or categories do not reveal specific mechanistic details. In addition, none of the steady-state analyses for DPD have considered the potential for dioxygen reactivity of reduced flavins ^{1, 2, 4-6, 19, 22, 28, 29, 31-35}.

In 1998, Rosenbaum et al. published transient state data for DPD that were consistent with a sequential rapid-equilibrium kinetic mechanism. This study measured ligand binding equilibria and included a preliminary examination of what was described as the transient state reductive half-reaction³⁰. The ligand binding data indicated low micromolar dissociation constants for uracil and NADPH. For the reductive reaction (carried out under anaerobic conditions) it was concluded that while NADPH binds and reduces the enzyme, the NADP+ formed was inhibitory and prevented the rapid reduction of the majority fraction of one flavin equivalent per protomer. In the presence of uracil, the reductive reaction was said to be approximately two orders of magnitude more rapid, leading to the conclusion that pyrimidine base occupancy at the FMN site enhances the capacity for hydride transfer at the FAD site (56 Å distant). The data from this study were not pursued in a systematic manner that would have enabled more substantial mechanistic conclusions to be drawn.

It therefore remains reasonable to state that the mechanistic understanding of DPD lags behind its therapeutic relevance and biochemical importance. Almost universally, traditional enzymological approaches based on aerobic steady-state turnover have been used to fashion a descriptive understanding of the kinetic mechanism. Here we show, using primarily transient state observations under anaerobic conditions (where appropriate), that DPD requires activation by two electrons from NADPH to constitute the catalytically active state of the enzyme. Importantly, this two-electron reduced form of DPD persists in the absence of NADPH and in the presence of pyrimidine substrate under anaerobic conditions. In the active state, occupancy of the pyrimidine and NADPH binding sites induces transmission of electrons from NADPH to the pyrimidine without evidence of the accumulation of an intervening reduced state of the enzyme. In the absence of the pyrimidine, DPD can be observed to reduce, but at a rate ~10 to 20-fold lower than the turnover number with native substrates.

Materials and Methods

Materials, quantitation and reaction conditions: Competent BL21 (DE3) cells were obtained from New England Biolabs. Tris(hydroxymethyl)aminomethane (Tris), dipotassium hydrogen phosphate (KPi), 5,6-dihydro uracil (DHU), 5,6-dihydro-5-methyluracil (DHT), ethylenediaminetetraacetic acid (EDTA), oxidized nicotinamide adenine dinucleotide phosphate (NADP⁺), ammonium sulfate, the Miller formulation of lysogeny broth (LB) powder, ammonium acetate, sodium dodecyl sulfate (SDS), methanol, acetonitrile and trichloroacetic acid were purchased from Fisher Scientific. Dithiothreitol (DTT) and reduced nicotinamide adenine dinucleotide phosphate (NADPH) were purchased from RPI Research Products. The sodium salt of ampicillin and dextrose powder were purchased from Spectrum Chemical. 5-Methyluracil (thymine), uracil (U), and glucose oxidase were obtained from Sigma-Millipore. Streptomycin sulfate powder was made by Gibco.

All concentrations of DPD substrates and products were determined spectrophotometrically using known extinction coefficients (NADPH; ϵ_{340} = 6,220 M⁻¹cm⁻¹, NADP+; ϵ_{260} = 17,800 M⁻¹cm⁻¹, uracil; ϵ_{260} = 8,200 M⁻¹cm⁻¹, dihydrouracil; ϵ_{225} = 1,280 M⁻¹cm⁻¹, thymine; ϵ_{264} = 7,860 M⁻¹cm⁻¹, dihydrothymine; ϵ_{225} = 1,670 M⁻¹cm⁻¹). All kinetic experiments were undertaken in reaction buffer (30 mM KPi, 2 mM DTT, pH 7.4) at 20 °C

Expression and purification of DPD: The methods for expression and purification of porcine DPD was from Beaupre et al.³⁶. The gene for porcine (*Sus scrofa*) dihydropyrimidine dehydrogenase (DPD) codon-optimized for heterologous expression in *E. coli* was synthesized and subcloned by Genscript. The gene was cloned into the expression plasmid pET17b utilizing the Nde I and Xho I

restriction sites. Mutation of this plasmid to produce a construct for expression of the C671S variant was also carried out by Genscript. The resulting plasmids, pSsDPD and pSsDPDC671S were transformed into *E. coli* BL21 DE3 cells, plated onto LB agar containing 100 μ g/mL ampicillin and grown for 16 hours at 37 °C. Cell stocks of WT and variant forms of DPD were prepared from an isolated colony used to inoculate ~20 mL of LB broth and cultured at 37 °C with 220 rpm agitation until early log phase growth was reached. Cells in broth were added to sterile glycerol (20 % final) and were aliquoted and stored at -80 °C.

Expression of both WT and variant forms of DPD was carried out by thawing a cell stock and spread plating 100 μ L onto LB agar, 100 μ g/mL ampicillin (2 plates per liter of culture) and incubation for 16 hours at 37 °C. The resulting cell lawn was suspended into LB broth using a plate spreader and was used to inoculate 1 L of pre-warmed LB broth, 100 μ g/mL ampicillin. Cell cultures were grown at 37 °C with shaking (220 rpm) until late log phase growth (OD_{600nm} = 0.6). The temperature was then decreased to 30 °C and left to equilibrate for 1 hour and then 100 μ M iron sulfate and 1 mM sodium sulfate was added. The culture was induced with 100 μ M isopropyl-0-1-thiogalactopyranoside and incubated at 30 °C with shaking for an additional ~20 hours.

All purification steps were undertaken at 4 °C. Cell cultures were harvested by centrifugation (4000 g for 30 min) and resuspended in 30 mM Tris, 2 mM DTT, pH 8.0 (buffer A,~20 mL per L of culture) and placed in a stainless-steel beaker. Before sonication, FAD and FMN were each added to a final concentration of 50 μ M. The slurry was then lysed with two 4 min periods of sonication using a Branson 450 sonifier set to provide 50 W of power. Lysed cells were centrifuged at 10,000 g for 45 min to pellet the cell debris. The crude supernatant was fractionated with ammonium sulfate and centrifuged at 10,000 g for 15 min. DPD was observed

to precipitate between 35% and 55% ammonium sulfate saturation. The 55% ammonium sulfate pellet was re-dissolved in buffer A and diluted until conductivity was equal to or less than 6 mS. The dilute crude sample was loaded at 1 mL/min onto a 2.5 x 20 cm High Q support anion exchange column (Bio-Rad) that had been pre-equilibrated in buffer A. The column was then washed with 200 mL of buffer A before fractionation using a 400 mL gradient from 0 to 300 mM NaCl in buffer A. Eluted protein was collected as 5 mL fractions. Fractions containing DPD were pooled and concentrated using a 10 kDa nominal molecular weight cutoff centrifugal concentrator (Millipore, Amicon) until the volume was equal to or less than 2 mL. The concentrated sample was then subject to size exclusion chromatography by loading onto a 2.5 x 100 cm Sephacryl S-200, high resolution column (Pharmacia Biotech) equilibrated with 30 mM Tris, 2 mM DTT, pH 8.0. DPD was eluted with 200 mL of 30 mM KPi, 2 mM DTT, pH 7.4 (reaction buffer) and collected as 5 mL fractions. Fractions that contained pure DPD (as judged by a 280 nm:380 nm absorbance ratio of \leq 3.5) were pooled, and concentrated. The enzyme was quantified using an extinction coefficient at 426 nm of 75,000 M⁻¹cm^{-1 36}. Aliquots of purified, concentrated DPD were stored at -80 °C.

Anaerobic methods for transient state observations: All transient state observations were made using a TgK stopped-flow instrument equipped with ceramic valves and PEEK flow circuit. A 1:1 mixing ratio and a 1 cm pathlength was used for all experiments. All stated concentrations pertaining to transient state observations are post mixing. The instrument was made anaerobic by the introduction of an anaerobic solution of 20 mM KPi, 10 mM dextrose pH 7.0 with glucose oxidase (10 U/mL) for a minimum of three hours prior to experiments. Enzyme solutions were

prepared anaerobically in tonometers and other glass vessels attached to a Schlenck line. Enzyme solutions were subject to 36 alternating cycles of mild vacuum (~730 mmHg) and 5 psi argon. Glucose oxidase (1 U/mL) was added from the sidearm of the tonometer. Tonometers were then mounted onto the stopped-flow instrument and mixed with substrate solutions. Anaerobic substrate solutions in reaction buffer contained 1 mM dextrose and were made anaerobic by sparging with purified argon gas for five minutes at which time 1 U/mL glucose oxidase was added and the sample mounted to the stopped-flow instrument ³⁷.

Steady-state Assay methods: Aerobic steady-state kinetics for DPD were determined under saturating conditions of pyrimidine (200 μ M) or NADPH (200 μ M) while varying the other substrate. All aerobic spectrophotometric assays were monitored with a Shimadzu UV-2600 spectrophotometer and were carried out at 20 °C in reaction buffer. Assays were initiated with the addition of DPD (0.4-1.5 μ M). Reactions where quantified by observing the oxidation of NADPH at 340 nm over a period of 200 seconds, the linear rate of which was typically measured between 20 and 60 seconds.

Anaerobic steady-state parameters were measured using a stopped-flow spectrophotometer. DPD (0.92 μ M) was prepared anaerobically in a tonometer. The enzyme and substrates were then combined by rapid mixing and the oxidation of NADPH observed at 340 nm and fit as above to determine rates. In these experiments, one of the two substrates was varied whilst the other was held constant and saturating. The saturating concentrations used were 75 μ M U and 112 μ M NADPH.

Dioxygen was also assessed as an oxidant in the steady-state. In this case the rate of turnover was measured using a Clark-type Hansetech Oxygraph electrode. The low rate of oxygen reactivity necessitated the use of relatively high DPD concentrations (4.5 μ M). The 1 mL reaction contained NADPH (0-1 mM) in the presence or absence of 250 μ M U and the reaction was monitored for oxygen consumption over 200 seconds. All assays were carried out under aerobic conditions (~250 μ M O₂) at 20 °C in reaction buffer. Steady state rates were measured from the data collected in the first 35 seconds.

For each steady-state experiment, the Michaelis constant (K_m) and the turnover number (k_{cat}) were determined from the fit of the initial rate dependence data to the Michaelis-Menten equation (Equation 1). To avoid unnecessary propogation of errors, the catalytic efficiency (k_{cat}/K_m) was calculated from a modified version of the Michaelis-Menten equation (Equation 2). All steady-state data dependencies were fit using the Marquardt-Levenberg least-squares routine available in KaleidaGraph Software (Synergy).

Equation 1.

$$\frac{v}{e} = \frac{k_{cat}[S]}{K_m + [S]}$$

Equation 2.

$$\frac{v}{e} = \frac{k_{cat}[S]}{k_{cat}} + [S]$$

Evaluation of DPD Reaction Thermodynamics: The equilibrium position of the DPD reaction was assessed in the forward (U or T and NADPH) and the reverse (DHU or DHT and NADP $^+$) directions. The assessment was made under anaerobic conditions monitoring the consumption or formation of NADPH at 340 nm. DPD (2.43 μM for U:NADPH and for T:NADPH) was prepared anaerobically in a tonometer in a solution of reaction buffer with 1 mM dextrose. Glucose oxidase (1 U/mL) was added from the tonometer side arm prior to mounting on the stopped-flow instrument. Substrate concentrations were each 100 μM and were prepared in reaction buffer anaerobically as described above and mounted to the stopped-flow instrument. After mixing, absorbance traces were recorded at 340 nm until the changes in absorption ceased ($^\sim$ 2000 seconds). The data reported from these experiments were the average of three observations.

Ligand Binding Isotherms: Binding isotherms for DPD substrate and product ligands were based on perturbation of the absorption spectrum of DPD. DPD was titrated with ligand and the absorption spectra between 250 and 850 nm were recorded using a Shimadzu-2600 spectrophotometer. All spectra were corrected for dilution and the fractional changes in the absorption at 500 nm were used as a measure of the DPD•ligand ([DPD•L]) concentration. The changes in absorption were fit to the quadratic form of the single site binding equation (Equation 4) in which [DPD] is the DPD concentration, [L] is the ligand concentration, K_L is the dissociation constant of the DPD•ligand complex.

Equation 3.
$$[DPD \bullet L] = \frac{t[L] + [DPD] + K_L) - \overline{t[L] + [DPD] + K_L)^2 - t4[L] + [DPD]}}{D}$$

The Reaction of DPD with NADPH in the Absence of Pyrimidine: The pyrimidine independent reaction of DPD with NADPH under anaerobic conditions was observed using stopped-flow spectrophotometry. DPD in reaction buffer with 1 mM dextrose was prepared in a tonometer as described above. This solution was then mixed with varied concentrations of NADPH (1 to 256 μ M) also prepared anaerobically. The solutions were mixed and the reduction of the cofactors of DPD was monitored at 440 nm. Data obtained from pseudo-first order reactant ratios were fit to a linear combination of two exponentials according to Equation 4, where k_{obs1} and k_{obs2} are the respective observed rate constants for the two phases, ΔA_1 and ΔA_2 are the amplitudes associated with each rate constant, and C is the absorbance endpoint.

Equation 4
$$A_{Xnm} = \Delta A_1 t e^{-k_{oLS1}t} + \Delta A_D t e^{-k_{oLS2}t} + C$$

Single Turnover with Limiting NADPH: Single-turnover experiments in the presence of excess saturating pyrimidine and limiting NADPH with respect to the enzyme concentration, were carried out under anaerobic conditions using stopped-flow methods. Reactions were monitored by absorption using either a charge coupled device (CCD) to gather spectra between 300 and 800 nm or by photomultiplier at 340 or 450 nm. For single-wavelength detection these positions primarily report absorption changes associated with NADPH and DPD respectively. In these experiments a tonometer containing wild-type or the C671S variant of DPD in reaction buffer with 1 mM dextrose was made anaerobic as described above and mounted onto the stopped-flow spectrophotometer. Kinetic data were the average of three observations. Reactions monitored using the CCD were collected for both short and long time-bases to obtain optimal

time resolution for successive fast and slow steps. Data were averaged from five separate observations for both time frames. These data were then stitched together into one dataset using excel software (Microsoft Corp.). The CCD data were analyzed using the SpectraFit singular value decomposition (SVD) routine available within KinTek Explorer Software (KinTek Ltd). The model free eigenvectors were used to conform the data to the minimal model shown in Scheme 3 that describes three species and two successive irreversible events, by eliminating the portion of the data deemed to be noise. In this scheme the first step represents the activation of the enzyme the second step represents the concomitant consumption of NADPH and formation of dihydropyrimidine. None of the complexity associated with the exchange of ligands between these states was included as these data contain only evidence of two first order events.

DPD·NADPH·PYR
$$\xrightarrow{k_{act}}$$
 DPD*·NADP·PYR $\xrightarrow{k_{cat}}$ DPD*·NADP·DHPYR Scheme 3

Turnover with Limiting Pyrimidine: Transient state analysis of NADPH oxidation in the presence of limiting uracil was used to assess the dependence of the amplitudes of both phases observed at 340 nm on the pyrimidine concentration. A solution of DPD C671S variant in reaction buffer with 1 mM dextrose was prepared anaerobically as described above and mounted onto the stopped-flow spectrophotometer. Multiple concentrations of limiting uracil (5 to 40 μM) were prepared anaerobically in reaction buffer containing 1 mM dextrose and 50 μM NADPH as described above. The solutions containing the substrates were mounted to the instrument and mixed with the enzyme. Reactions were monitored at 340 nm following the absorption changes

relative to the NADPH oxidation extinction coefficient change (6,220 M⁻¹cm⁻¹). The amount of NADPH oxidized in each phase was estimated from the amplitudes of the absorbance changes of both phases.

HPLC Stoichiometric Analysis of Single-Turnover Reactions with Limiting NADPH: Stoichiometry of NADPH oxidation and pyrimidine reduction (uracil or thymine) during each phase of the events observed in single-turnover reactions was assessed using the C671S variant as this form of the enzyme exhibits marked separation of what are described here as successive activation and catalytic phases. HPLC product analysis conducted after the reactions were quenched at predetermined timepoints (10, 100 and 600 seconds for uracil and 10 and 80,000 seconds for thymine) was used to assess relative NADPH and pyrimidine consumption. A solution representative of time zero was made by substituting the addition of DPD with reaction buffer. This experiment used reactant ratios that support both activation and subsequent single turnover (C671S DPD (50 μ M), thymine or uracil (80 μ M) and NADPH (40 μ M)). The reaction also included an inert internal standard of tryptophan (100 µM) to allow normalization of the HPLC data. With the exception of the longest time point for thymine (which was prepared in a more an anaerobic cuvette), the reaction was prepared in an anaerobic vessel with a port covered by a rubber septum. Enzyme in reaction buffer with 1 mM dextrose was made prepared as described above. After anaerobic conditions were achieved, glucose oxidase (1 U/mL) was added to remove any residual oxygen. The reaction was initiated by the injection of 250 µL of an anaerobic solution giving a final concentration of 40 μM NADPH, 80 μM pyrimidine and 100 μM tryptophan. To terminate the reaction at the desired time, magnetic stirring was initiated and a 1:1 ratio of anaerobic 1M trichloroacetic acid with 1 mM EDTA was added to the reaction vessel via the septum. The substrate and acid solution were made anaerobic by sparging with pure argon for 5 5 minutes as described above. The samples were then removed from the vessel, vortexed for 2 minutes, and then centrifuged for 10 minutes at 10,000 g at 4 $^\circ$ C to pellet the denatured enzyme. The supernatant was collected and neutralized by titration with 3M NaOH until a pH of 7 7 was recorded on litmus paper and immediately frozen at $^-80$ $^\circ$ C. A 20 μ L aliquot was injected onto a C18 column (Xterra 5 μ m, 4.6 x 250 mm) pre-equilibrated in 10 mM ammonium acetate, 15 mM triethylamine with 1 % acetonitrile, pH 6.5 (titrated with acetic acid). The sample was eluted under isocratic conditions at 1 mL/min and monitored simultaneously at 260 and 300 nm. On the day of analysis, a standard curve was acquired for NADP+, tryptophan, and pyrimidine (thymine or uracil) and the linear dependencies were used to quantify the amount of NADPH oxidized and pyrimidine reduced during the reaction. Dihydrothymine and dihydrouracil were not quantified due to their low extinction coefficients in the near-UV region of the spectrum. NADPH was not quantified due to denaturation in acid.

Results

Steady-state Kinetics: In this study steady state kinetic experiments were used primarily to compare apparent k_{cat} values to the rate constants measured in transient state experiments. Table 1 summarizes steady-state kinetics observed for WT and the C671S variant of DPD. These data indicate k_{cat} and K_m values for the WT that are comparable to those previously published for the porcine homolog³⁴.

aerobic					anaerobic						dioxygen consumption	
	WT DPD			C671S DPD	WT DPD			C671S DPD			WT DPD	
	NADP H (200 μM U)	Uracil (200 μM NADPH)	Thymine (200 µM NADPH	Uracil (200 µM NADPH)	NADPH (75 μM U)	Uracil (112 μΜ NADPH)	Thymine (200 µM NADPH)	NADPH (100 μM U)	Uracil (150 µM NADPH)	Thymine (150 μΜ NADPH)	NADPH (250 μM O ₂)	NADPH (250 μM O ₂ , 250 μM U)
k _{cat} (s ⁻¹)	0.65 ±0.01	0.73 ±0.01	0.42 ±0.02	0.030 ±0.001	0.85 ±0.01	0.78 ±0.01	0.39 ±0.01	0.015 ±0.001	0.015 ±0.001	0.00024*	0.043 ±0.001	0.015 ±0.003
K _m (μM)	5.4 ±0.7	6.3 ±0.7	4.6 ±0.6	1.48 ±0.35	2.3 ±0.09	0.87 ±0.5	0.79 ±0.1	9.31 ±0.02	5.48 ±0.09	NM	NM	NM
K _{cat} /K _m (μΜ ⁻¹ s ⁻¹)	0.12 ±0.01	0.11 ±0.01	0.09 ±0.01	0.02 ±0.01	0.36 ±0.08	0.90 ±0.08	0.50 ±0.07	0.002 ±0.001	0.003 ±0.001	NM	NM	NM

*taken from Figure 5, NM - not measured

Table 1. Apparent steady state parameters of wild type DPD and C671S variant DPD.

The steady-state parameters were similar when comparing those data collected under anaerobic and aerobic conditions, suggesting that dioxygen is not a significant oxidant for reduced forms of DPD in the presence of native substrates. Using dioxygen as the exclusive oxidant revealed a rate of turnover $\sim 1/17^{\text{th}}$ that observed with uracil as the oxidant. In addition, the consumption of dioxygen was suppressed by three-fold when excess uracil was added to the reaction, suggesting that electrons lost to dioxygen most often exit the enzyme through the FMN cofactor. This indicates that DPD is relatively unreactive with dioxygen and that prior steady-state observations made in atmosphere were not significantly undermined by loss of electrons via this route^{1, 2, 4-6, 19, 22, 28, 29, 31-35}. The k_{cat} values are of prime relevance to this study as we have previously demonstrated that the enzyme is fully active and the turnover number will therefore correspond

with the slowest step(s) observed in transient state³⁶. For the wild type enzyme this value was observed to be ~0.8 s⁻¹ with uracil and ~0.4 s⁻¹ for thymine. The k_{cat} of the C671S variant was significantly lower and was more dependent on the identity of the oxidant substrate in that the k_{cat} with thymine, estimated at 0.00024 s⁻¹ is ~60-fold lower than that with uracil at 0.015 s⁻¹.

Thermodynamic Evaluation of the DPD Reaction: While it is widely reported that the DPD reaction is reversible ¹⁻⁵, the free energy change of the reaction has not been previously determined. Such a determination requires strict anaerobic conditions to avoid skewing the measurement by incorporating the highly endergonic reduction of dioxygen. To measure the equilibrium position of the DPD reaction equimolar concentrations of pyrimidines and NADPH or dihydropyrimidines and NADP+ were combined under anaerobic conditions and the consumption or production of NADPH was observed (Figure 2).

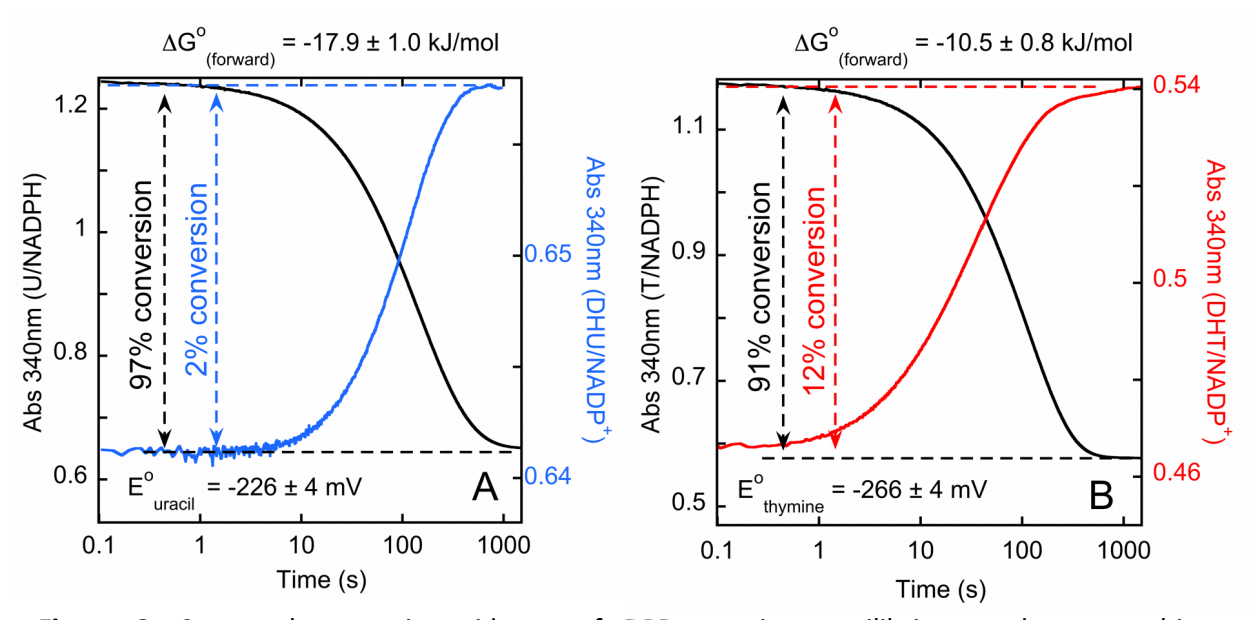


Figure 2. Spectrophotometric evidence of DPD reaction equilibrium under anaerobic conditions. **A.** DPD (2.43 μ M) was combined in a stopped-flow spectrophotometer with either 100 μ M of both NADPH and uracil (black) or NADP+ and dihydrouracil (blue). **B.** DPD (2.43 μ M) was combined in a stopped-flow spectrophotometer with either 100 μ M of both NADPH and thymine (black) or NADP+ and dihydrothymine (red). Data for both reactions was recorded at 340 nm for 2000 seconds. Each trace is the average of three observations.

For the U:NADPH reaction, the forward reaction was observed to be 97% converted at equilibrium. Similarly, for the reverse reaction, equilibrium was attained at 2% completion. These data indicate that the average ΔG° of the U:NADPH reaction in the forward direction is -17.9 \pm 1.0 kJ/mol and that the two-electron reduction potential of the U:DHU couple is -226 \pm 4 mV. For the T:NADPH reaction the forward reaction was observed to be 91% converted at equilibrium and for the reverse reaction equilibrium was attained at 12% completion. These data indicate that the average ΔG° of the T:NADPH reaction in the forward direction is -10.5 \pm 0.8 kJ/mol and that the two-electron reduction potential of the T:DHT couple is -266 \pm 4 mV. These values compare favorably with the ΔG° of -13.3 kJ/mol for the reaction in the same direction of dihydroorotate dehydrogenase and the orotate:dihydroorotate couple of -252 mV determined by Krakow and Vennesland ³⁸. Sources of additional error in this data arise from changes in the

spectrum of the enzyme that occur with pre-activation (see below) and varied spectral perturbation as the pyrimidine:dihydropyrimidine ratio changes. This latter complication is not significant for T/DHT but may be a small source of error for U/DHU (see Figure 3 below).

Ligand Binding Isotherms: The association of substrate and product ligands perturbs the DPD absorption spectrum providing a simple means of measuring dissociation constants for the enzyme. These values were used to define saturating ligand concentrations in transient state experiments. The K_d values measured for oxidized DPD indicate low micromolar binding for substrate pyrimidines and 4 to 20-fold weaker binding for dihydropyrimidines (Figure 3). NADP+ is also observed to bind to DPD with high affinity, with a K_d of 1.6 μM (data not shown). This K_d is consistent with prior reports that show DPD reduction is hindered by NADP+ that accumulates with oxidation of NADPH and that this inhibition can be alleviated to some degree by the addition of an enzyme that reduces NADP+ to NADPH³⁰.

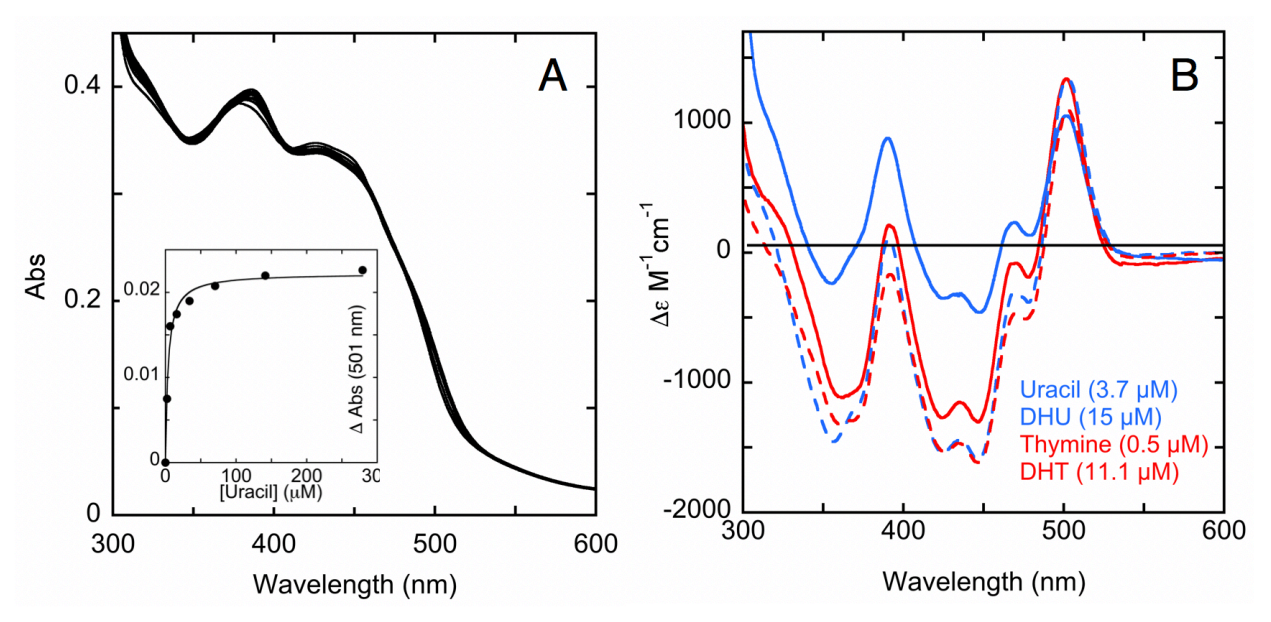


Figure 3. Ligand dissociation constants for DPD. Ligand dissociation constants were determined from perturbation of the DPD spectrum. **A.** Example titration of 4.5 μ M DPD with uracil (0 – 256 μ M). Inset depicts the change in absorbance at 501 nm plotted against the concentration of uracil and fit to Equation 3. **B.** The binding difference spectra observed for saturating ligands associating with DPD. Dissociation constants for the DPD•L complexes are shown in the bottom right. Uracil and thymine are depicted with solid lines while their respective products are shown in dashed lines.

Reduction of WT DPD by NADPH in the Absence of Pyrimidines: For flavoprotein dehydrogenases, it is generally possible to observe reduction of the flavin by NADPH independently by excluding the oxidizing substrate (and dioxygen). For DPD, the reduction of the enzyme was evident as modest extinction coefficient changes between 380 and 460 nm upon titration of NADPH under anaerobic conditions (Figure 4). The kinetic traces for 440 nm that were pseudo-first-order with respect to the concentration of the enzyme were fit to Equation 4. The fit to this equation returned a $k_{obs1} = 2 \text{ s}^{-1}$ for the initial phase followed by a slower phase with a rate constant $k_{obs2} = 0.04 \text{ s}^{-1}$. This latter phase accounted for ~75% of the overall amplitude change at 440 nm. The slow phase is 10 to 20-fold lower than the observed turnover number and thus is not catalytically relevant. The overall change in extinction coefficient for both phases was

~ 6,500 M⁻¹cm⁻¹, approximately equivalent to the reduction of one flavin per subunit at this wavelength. The extent of the reaction titrated with NADPH concentration indicating an equilibrium reduction process.

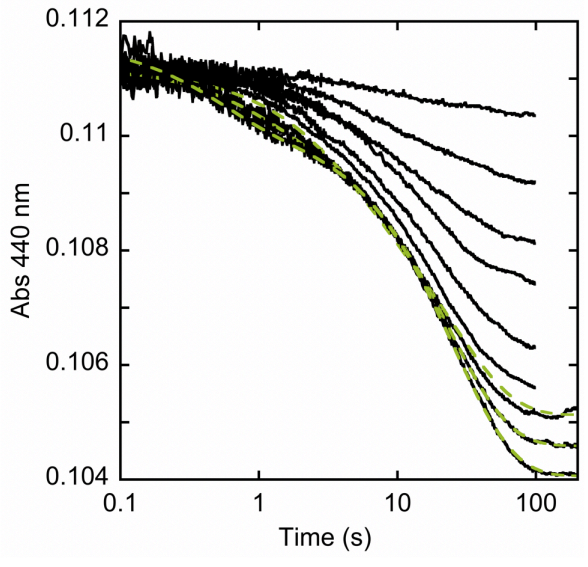


Figure 4. Wild-type DPD reacting with NADPH under anaerobic conditions. Reduction of 1.7 μM DPD when titrated with NADPH monitored at 440 nm. Traces shown top to bottom are for 1, 2, 4, 8, 16, 32, 64, 128, and 256 μM NADPH. Data for NADPH concentrations that were pseudo first order to the enzyme concentration (64, 128 and 256 μM) were fit to Equation 4.

Single-Turnover Analysis of DPD WT and the C671S Variant: Turnover of DPD in the presence of saturating oxidant pyrimidine and limiting NADPH with respect to the enzyme concentration was monitored at 340 nm using photomultiplier and/or using CCD detection (Figure 5). In all experiments, observation at 340 nm reveals two phases of decreasing absorption, similar to those seen in reductive half reaction experiments in the absence of the pyrimidine (Figure 4).

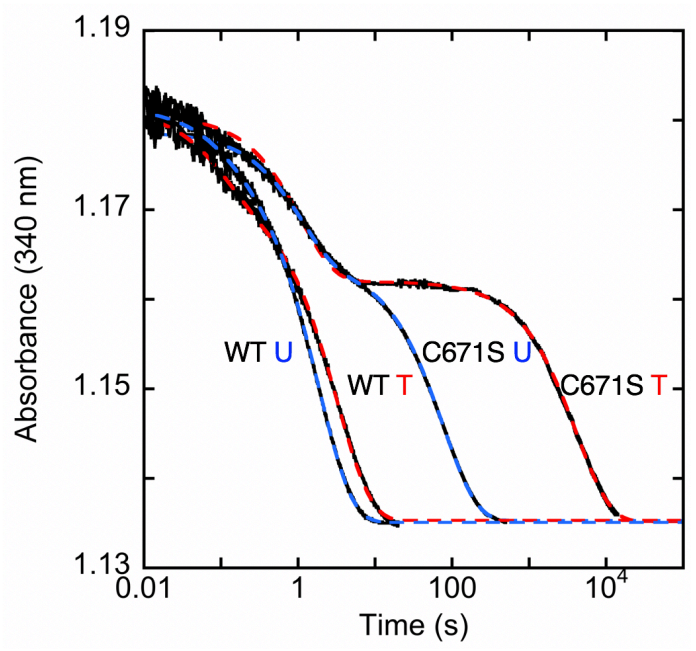
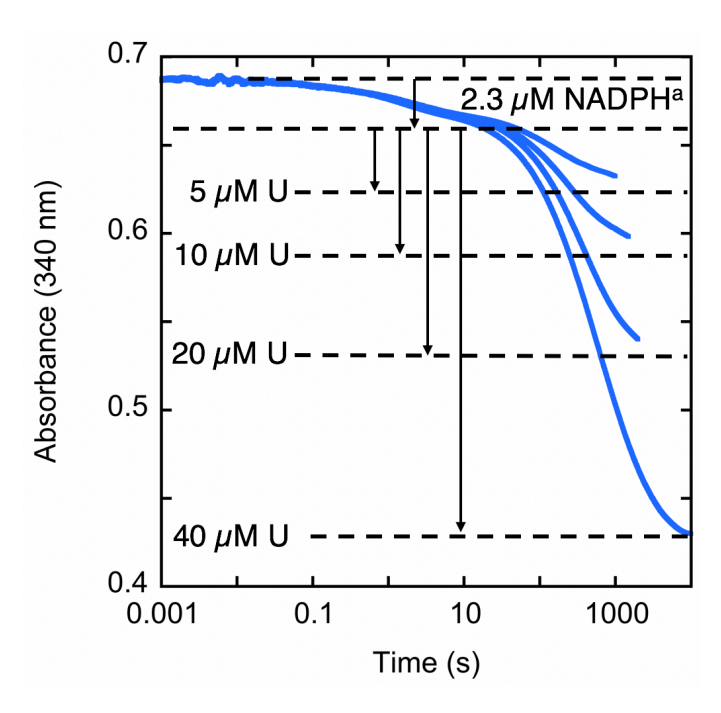


Figure 5. Comparison of Net Single-Turnover reactions of the WT and C671S variant DPDs, monitored at 340 nm under anaerobic conditions. Amplitudes of reaction traces were normalized to equate to 10 μM NADPH consumption. The data were fit to Equation 4 to derive estimates of the rate constants for the two phases observed. Fits are shown as individually colored dashed lines. The actual concentrations used were as follows: WT U, 12.8 μM DPD, 100 μM uracil, 7.5 μM NADPH, WT T, 12.8 μM DPD, 100 μM thymine, 7.5 μM NADPH, C671S U, 12.0 μM DPD, 100 μM uracil, 9.6 μM NADPH, C671S T, 12.0 μM DPD, 100 μM thymine, 10.0 μM NADPH.

In Figure 5, the dependence of the two phases observed in single turnover with limiting NADPH on the form of the enzyme and the substrate are compared. These data show that the rate of the first phase is dependent on the enzyme form (WT vs C671S) and that the rate of the second phase is dependent both on the form of the enzyme and on the pyrimidine substrate (U vs T). When fit to Equation 4, the first phase for the WT enzyme returned an average rate constant of $9.0 \pm 0.7 \, \text{s}^{-1}$. The first phase for the C671S variant enzyme fit to the same equation gave a rate constant ten-fold lower at $0.91 \pm 0.01 \, \text{s}^{-1}$. The second phase returned rate constants that indicate a greater dependence on the identity of the substrate pyrimidine. For WT DPD this phase was fit to $0.54 \pm 0.01 \, \text{s}^{-1}$ for uracil, while for thymine the fit returned a value approximately two-fold lower of $0.31 \pm 0.01 \, \text{s}^{-1}$. The latter of these values qualitatively agrees with the measured turnover number for this substrate with the WT enzyme (Table 1). The ~30% discrepancy in the measured rate constant and the k_{cat} value for the uracil substrate is likely a limitation of analytical fitting to exponentials. The fact that the two events captured in this trace are poorly delineated

dictates that the confidence interval of the rate constants will be large relative to the fit error. When fixed to match the k_{cat} value measured in the steady state, the fit conforms to the line, but returns greater error for the parameters determined. For the C671S variant the second phase was fit to rate constants of $0.013 \pm 0.001 \, \text{s}^{-1}$ and $0.00024 \pm 0.00001 \, \text{s}^{-1}$ for uracil and thymine respectively; the former of which correlates well to the measured turnover number (Table 1). Interestingly, the turnover number for this variant measured under aerobic conditions is additive with the aerobic rate of dioxygen consumption in the presence of uracil for the WT enzyme, suggesting that the apparent aerobic turnover number (based on NADPH oxidation) for this variant is elevated by the reduction of dioxygen. These data show a 55-fold influence of the variant serine the the thymine substrate, considerably larger than the dependence observed for the WT enzyme.



Dependence Figure pyrimidine concentration the observed amplitude of the second phase. DPD C671S variant (4.2 μM) with NADPH (50 μM) was titrated with uracil (5, 10, 20, 40 μM) monitored at 340 nm. ^aThe amplitudes of both phases of each trace are evaluated relative the extinction to coefficient change for the oxidation of NADPH (6,220 M-¹cm⁻¹) indicated as dashed lines.

In Figure 6 the amplitudes of the two phases observed were evaluated with respect to limiting pyrimidine concentration. In this experiment each uracil concentration was limiting and

the amplitudes of the second phase titrated with the pyrimidine concentration indicating that uracil reduction is occurring in this phase. These traces do not end cleanly due to the ensuing slow reduction of the enzyme in the presence of excess NADPH (Figure 4) and so the traces were truncated to an early indication of slowing curvature. Data of this type was observed previously by Rosenbaum et al. ³⁰. The purpose of this experiment is demonstrative and so the data were not fit either analytically or to an encompassing model. The first phase is unchanging for each uracil concentration indicating that the amplitude and rate constant of this phase is independent of the uracil concentration. Together these observations indicate that only the second phase includes reduction of the pyrimidine substrate.

In order to define the net spectrophotometric changes occurring in each the observed phases in single-turnover reactions, the C671S variant of DPD was mixed with saturating uracil and limiting NADPH and time-dependent spectral data were collected using CCD.

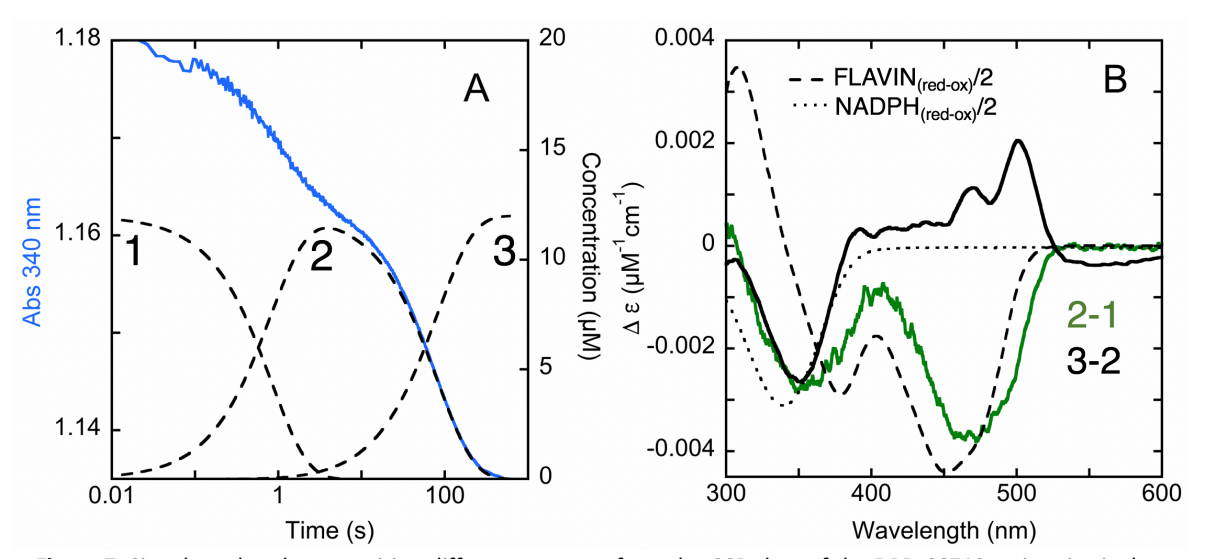


Figure 7. Singular value decomposition difference spectra from the CCD data of the DPD C671S variant in single turnover. A. Representative single wavelength trace (340 nm). The C671S variant DPD (12 μ M) was mixed with saturating uracil (100 μ M) and limiting NADPH (10 μ M) and monitored using CCD. B. Difference spectra computed from SVD deconvoluted data from CCD for species indicated as 1, 2, and 3 in A. The positions of these numbers correspond to the time of maximal concentration of each species as shown. Reference spectra for assignment of difference spectrum 2-1 are overlaid in B. These are one half equivalent for reduction of a flavin (dashes) and oxidation of one half equivalent NADPH (dots).

This experiment used the variant form of the enzyme as the two phases under study are more clearly delineated (Figure 5). Moreover, the single-turnover kinetics observed for the C671S variant with uracil is more amenable to observation within the timescales available for the stopped-flow instrument compared to the kinetics of the reaction with thymine. This dataset was deconvoluted using SVD analysis which resulted in clearly resolved spectra for each of the three species observed. The deconvoluted spectra were used to calculate difference spectra representing the net absorption changes in both phases. The difference spectrum representative of the changes that occur in first phase (2-1 in Figure 7) indicates a decrease in extinction coefficient of ~2,800 M⁻¹cm⁻¹ at 340 nm and ~3,700 M⁻¹cm⁻¹ at 480 nm. Both of these changes are consistent with partial reduction of DPD in the first phase. Furthermore, the difference spectrum is similar in shape and intensity to one half the difference spectrum for reduction of a red-shifted flavin isoalloxazine, accounting for reduction of one flavin per dimer. The difference spectrum of the second phase (3-2 in Figure 7B) has characteristics that represent the spectral properties of both pyrimidine ligand association at 500 nm (Figure 3) and NADPH oxidation at 340 nm. Interestingly the magnitude of the change at 340 nm is similar to that observed in the first phase (2-1). This was interpreted as the difference-difference spectrum of uracil vs dihydrouracil binding that arises as this product is formed in this phase. When the final spectrum is subtracted from the initial (3-1) the difference in extinction coefficient change at 340 nm is consistent with the overall oxidation of NADPH (10 μ M) expected in this reaction (not shown). However, that half this concentration was consumed in the first phase, suggests that a reductive activation of the enzyme precedes catalytic turnover. In addition, the spectral change centered around 480 nm in the first phase (2-1) does not have an equivalent opposite change in the

subsequent phase (3-2) even in the presence of excess uracil. This reveals that the changes imparted in the first phase remain in the final state, suggesting that the redox state of the enzyme at position 2 is the same as at position 3.

Figure 8A shows four single-turnover traces at 340 nm for the C671S variant reacting with excess saturating uracil and four concentrations of NADPH, each less than the enzyme concentration.

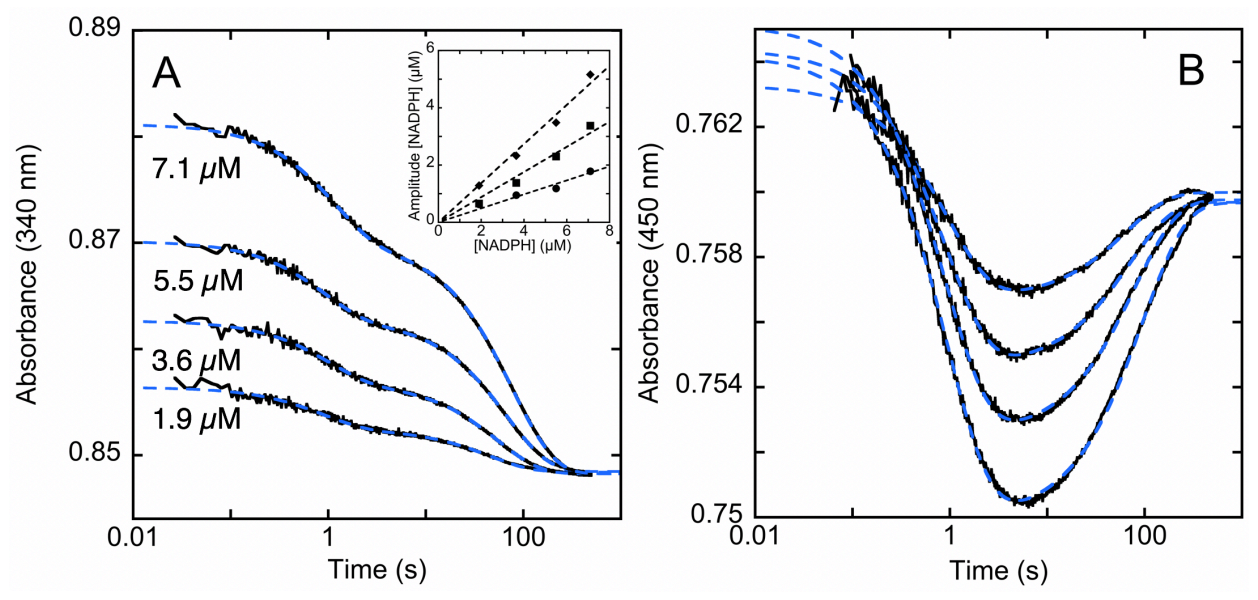


Figure 8. C671S variant DPD single turnover varying NADPH. A. DPD C671S variant (8.8 μ M) with uracil (100 μ M) titrating NADPH (as labeled) monitored at 340 nm. Traces were fit to a linear combination of 2 exponentials as described by Equation 4. Inset. Amplitudes of phases 1 (circles) and 2 (squares) and sum of both traces (diamond) from the fit of traces in plot A to Equation 4. B. Data from the same experiment collected at 450 nm, fit to Equation 4. For exposition of the data, both data sets were artificially adjusted to end at a common absorption value.

The data show two phases for each concentration of NADPH and were fit to Equation 4 to assess the relative amplitudes of each phase. The rate constants determined for each trace were $^{\sim}1 \text{ s}^{-1}$ and 0.015 s $^{-1}$ in agreement with prior experiments (Figures 6 & 7, Table 1). That neither rate constant titrates with NADPH concentration indicates that the data is not influenced by a prior equilibrium associated with binding and therefore that the affinity for this substrate is high. The ratio of the observed amplitudes is consistently 0.56 (Amp 1/Amp 2), suggesting either that the

concentration of NADPH oxidized is different for each phase or that underlying absorption changes from the protein chromophores diminish or increase one or both of the observed amplitudes. Accordingly, when the sum of the amplitudes (in μM) is plotted against NADPH concentration the slope is 0.68, definitively indicating other concomitant processes decrease the overall amplitude observed by 30%. Evidence for concomitant spectrophotometric changes associated with the protein can be seen in Figure 8B for the same concentration series but observed at 450 nm, beyond the contribution of NADPH. These traces can be fit to the same rate constants derived from the fit in Figure 8A (~1 s⁻¹ and 0.015 s⁻¹). This figure shows that the first phase observed in Figure 8A corresponds to a decrease at 450 nm that is also proportional in amplitude to the NADPH concentration and consistent with reduction of a flavin. The ensuing event observed at this wavelength is an increase in absorption, but the amplitude observed does not return the enzyme to the value observed at the initial state, added evidence that the chemistry of the first phase fundamentally changes the enzyme. Correlation with the data from Figure 7 indicates that this phase also includes ligand binding perturbation differences between the uracil and dihydrouracil that arise during pyrimidine reduction (Figure 3).

In order to establish exact stoichiometries of NADPH consumption and pyrimidine reduction, acid quench experiments were conducted for single-turnover reactions of the C671S variant reacting with excess pyrimidines and limiting NADPH under anaerobic conditions. The reactions were quenched in trichloroacetic acid and returned to neutrality before HPLC analysis to quantify NADP+ formed and pyrimidine consumed at specific times. In Figure 9 single-turnover traces collected at 340 nm for limiting NADPH reactions for both pyrimidine substrates are included for reference. These analyses show for both uracil and thymine that the ratio of

NADPH:pyrimidine is 2:1. One half of the NADPH added is consumed in the first phase observed at 340 nm and reduction of pyrimidine occurs in the second phase during which time the remaining NADPH is oxidized. This convincingly shows that the first phase is a pre-activating reduction step that indicates, at a minimum, that the activated form of the enzyme is two-electron reduced on one subunit. Moreover, the data from Figure 7 indicate that electrons acquired during the first phase reside on a flavin cofactor and persist when the NADPH concentration is exhausted even in the presence of excess oxidant substrate.

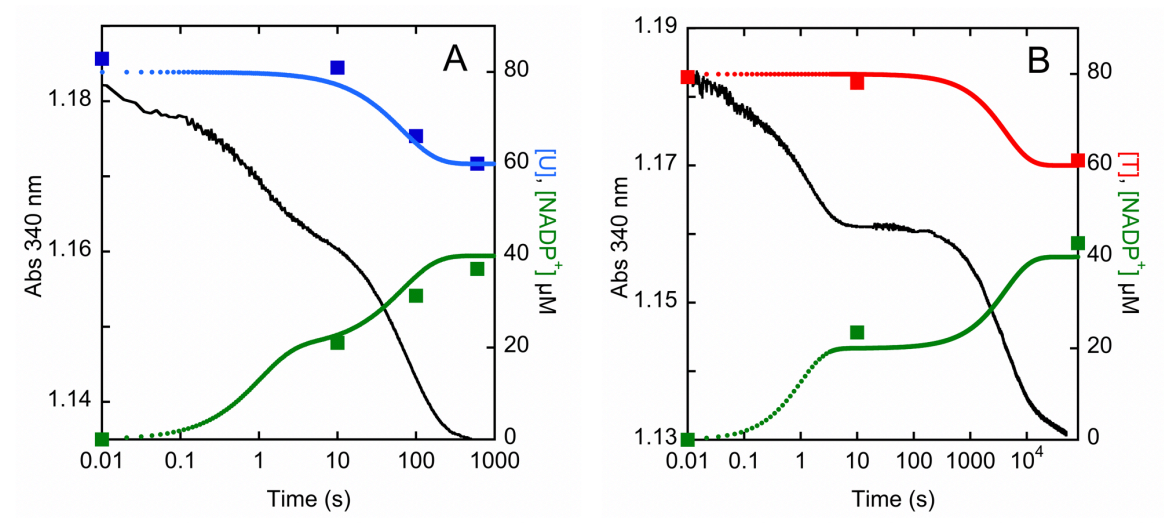


Figure 9. Acid quench HPLC analysis of C671S DPD single turnover reactions with uracil and thymine in the presence of limiting NADPH. **A.** DPD C671S variant (50 μ M) was combined with saturating uracil (80 μ M) and limiting NADPH (40 μ M). **B.** DPD C671S variant (50 μ M) was combined with saturating thymine (80 μ M) and limiting NADPH (40 μ M). Reactions were quenched in 1M TCA and 1 mM EDTA and neutralized. For each pyrimidine substrate the data from HPLC is overlayed with a single turnover reaction trace monitored at 340 nm with that substrate. These traces are added for correlation and are not derived from the same experiment. Theoretical curves for the accumulation of NADP+ and the consumption of pyrimidine are added to plots **A** & **B** to illustrate the predicted data for the 2:1 NADPH:pyrimidine ratio proposed for activation and subsequent turnover. Concentrations of pyrimidine substrates and NADP+ were determined at specific times. Points indicated at 0.01 seconds are from control samples quenched without the addition of enzyme and added as a reference representative of time zero.

Discussion

Dihydropyrimidine dehydrogenase catalyzes a relatively simple reaction involving two hydride transfers whose purpose is to reduce the pyrimidine bases uracil and thymine at the 5-6 vinylic bond to form dihydropyrimidine products (Scheme 1). This activity is the initial step in the degradation of pyrimidine bases and is analogous to the reaction catalyzed by dihydroorotate dehydrogenases (DHOD) that install the 5-6 vinylic bond during pyrimidine biosynthesis. Moreover, class 1a DHODs have the same topology as domain IV of DPD^{23, 27, 39}. The structure of DPD seemingly defies the simplicity of the chemistry catalyzed. Each protomer of the DPD headto-head homodimer has two substrate ligand binding sites each with a flavin cofactor and an apparent wire of four Fe₄S₄ centers that bridges the flavins (Figure 1). In nature, the type of chemistry catalyzed by DPD is more often achieved with a single flavin cofactor with sequential reductive and oxidative half-reactions (Scheme 2), as is the case for class 1a DHODs. DPD has been studied extensively, but it should be asserted that a basis for its structural complexity has not yet been offered. In this study we use the chromophoric nature of DPD, its substrates, and products to observe WT and a variant form of the enzyme in order to formulate a model for the kinetic mechanism from single-turnover reactions.

Prior steady state analysis of mammalian DPDs have indicated both ping pong and random sequential mechanisms^{5, 31}. In the case of DPD, these categories are not mutually exclusive as both substrates can and do add to the enzyme prior to catalysis and kinetic patterns consistent with a ping pong mechanism would be observed if an intervening reduced state of the enzyme were to accumulate. To some extent these prior studies highlight the extent to which traditional approaches fail to capture the complexity of two active sites linked by redox

chemistry. As such, in this study we defined the chemistry and kinetic mechanism of DPD using almost exclusively transient state approaches under anaerobic conditions. These methods capture individual rate constants and stoichiometries and were employed to provide a more detailed account of the chemistry at work. Initially anaerobic transient state experiments were used to define the energetics of the DPD reaction (Figure 2). Though the chemistry catalyzed by DPD has been consistently described as reversible^{1, 2, 28, 32, 35}, the degree of reversibility had hitherto not been measured. The data indicate that the reduction of pyrimidines is strongly favored to the degree that reversibility is not a significant factor in data analysis of the forward direction reaction, as depicted in Scheme 1.

Despite having eight Fe₄S₄ centers per dimer, mammalian DPD enzymes can be purified in the presence of dioxygen to yield viable enzyme ^{29, 36}. This establishes that the iron-sulfur centers are sequestered and stable to external oxidants. Evidence for this can also be seen in oxygen consumption experiments where decoupling to dioxygen reduction occurs only in one of ~17 turnovers in a process that does not irreversibly inactivate the enzyme (Table 1). The fact that saturating pyrimidine can suppress dioxygen reduction by DPD to ~65% implies that electrons derived from NADPH either reside at or can only exit the enzyme via the FMN cofactor. In Table 1 we observe that mutation of the pyrimidine site candidate general acid, C671, to a serine slows the turnover of the enzyme by approximately 60-fold for uracil and 1,600-fold for thymine. The data presented do not provide an explanation for the 31-fold relative difference for the thymine versus uracil turnover numbers of the WT and C671S variant. That the measured turnover numbers correlate well with the second phase observed in single-turnover reactions indicates that pyrimidine reduction is rate limiting in turnover (Figure 5). In the absence of pyrimidines and

the presence of ~250 μ M dioxygen, DPD reduces dioxygen at rates that are ~20-fold lower than the turnover number for uracil. This rate of turnover correlates directly to the apparent rate constant for reduction of DPD by NADPH in the absence of pyrimidine substrates (Table 1, Figure 4). This suggests that dioxygen reactivity is defined by the rate of reduction by NADPH. The data in Figure 4 were the initial indication that NADPH is oxidized by the enzyme at two rates. Characterization of these biphasic processes is the primary theme of the work presented.

The absolute requirement of the presence of the pyrimidine substrate for observation of catalytically relevant rates (Figure 4 vs Figure 5) meant that traditional approaches such as the observation of separate reductive and oxidative half reactions could not be pursued. We instead focused on the observation of single-turnover reactions with limiting substrate concentrations. In reactions where NADPH was limiting, two distinct phases are seen at 340 nm, a wavelength that captures, at a minimum, NADPH oxidation. The data shown in Figure 5 are included as justification for the predominant use of the C671S variant in this study. These data indicate that for both forms of the enzyme, the two phases are consistently observed. It also illustrates that the rate associated with the first phase is influenced by the form of the enzyme and the rate for the second phase is dependent both on the pyrimidine substrate and the enzyme form. The rates of the two phases with the C671S variant enzyme provide a means for delineated observation of these two events. The amplitude of the second phase is proportional to the concentration of added pyrimidine indicating that the catalytic turnover of DPD is occurring in this phase (Figure 6). The preceding phase exhibits no dependence in terms of rate constant or amplitude on the concentration of the pyrimidine substrate, suggesting that this phase is a pre-activating reduction step (Figure 6). Time dependent spectra recorded in single turnover with limiting NADPH and

analyzed by SVD, revealed the net absorption changes occurring in each phase observed. The difference spectrum for the first phase is consistent with both oxidation of NADPH and the reduction of a flavin at one protomer (Figure 7B). The difference spectrum for the second phase includes evidence of NADPH oxidation and spectral features associated with pyrimidine/dihydropyrimidine binding (Figure 7B vs Figure 3). Taken together, these spectra can be interpreted as phase one involving reduction of one of the two flavins of one subunit and phase two including further NADPH oxidation concomitant with reductive conversion of the pyrimidine substrate.

The net absorption changes at ~480 nm shown in Figure 7B are not consistent with reduction of one equivalent of a flavin in all DPD subunits. The change in extinction coefficient correlates only with the reduction of one flavin per DPD dimer (one half of ~7,600 M⁻¹cm⁻¹). Importantly, this change in absorption at ~480 nm remains in the spectrum when the NADPH is exhausted and in the presence of excess oxidant substrate, which is strong evidence that the first phase is reductive activation. One possible explanation for the inability of pyrimidine substrates to fully oxidize the activated enzyme can be found in the available crystal structures of DPD. In the structures of the porcine enzyme in complex with 5-iodouracil, the position of cysteine 671 is apparently contingent on the occupancy of the NADPH binding site (Figure 10). In the presence of NADPH, this cysteine is equidistant at 3.9 Å from the C5 and C6 positions of the base. While in the absence of NADPH the cysteine is ~9 Å distant from the pyrimidine ring ⁷. Taken together these data suggest a ligand gated conformational switch for C671 that accounts for the inability of pyrimidine to fully reoxidize activated DPD in the absence of NADPH in that the open complex does not complete the conduit for proton coupled electron transmission.

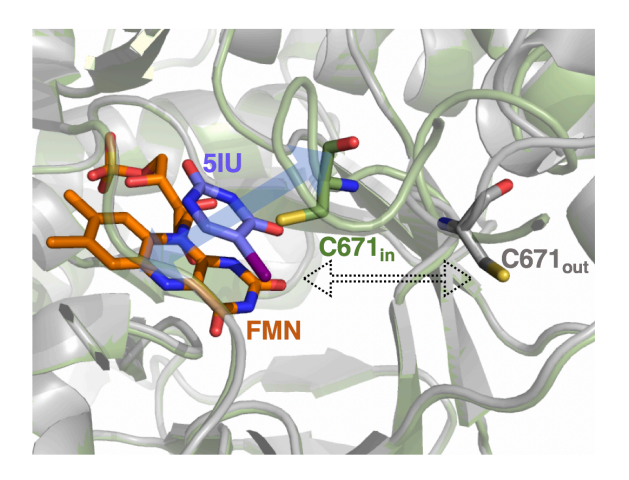


Figure 10. The observed positions of C671 in the presence of 5IU alone (PDB ID: 1GTE, grey) and 5IU with NADPH (PDB ID:1GTH, green).

One of the most confounding features of the activation and ensuing pyrimidine reduction proposal is seen in Figure 8A. Limiting concentrations of NADPH with respect to the enzyme concentration yield biphasic traces at 340 nm. If the first phase were simply reductive activation as proposed, it stands to reason that all of the NADPH would be consumed in the activation phase. Biphasic kinetics suggests that the subunit harboring the flavin that is reduced with activation is then committed to reduction of pyrimidine in the second phase before the other subunit of the dimer is activated. It is therefore reasonable to assume that the activated subunit has considerably increased affinity for NADPH, such that it exclusively captures and utilizes the remaining NADPH. This evidence limited the number of possible models that would account for the product analysis of the C671S variant in single turnover (Figure 9). Analysis indicated that the stoichiometry of the two successive phases for NADPH and pyrimidine is 2:1 with respect to the subunit concentration. Figure 11 shows a model that accounts for the stoichiometry observed and a simulation of the biphasic data shown in Figure 8A based on this model. The model requires that after activation, unreacted NADPH would exchange with NADP+ formed at the activated

subunit before reduction of the pyrimidine occurs. This model was used to recapitulate the data from Figure 8A as proof of concept and is not offered as a definitive fit to the data. The simulation includes numerous ligand binding equilibria that were not defined in the current work. With the exception of the binding of NADPH to the activated enzyme, undefined substrate binding equilibria were arbitrarily fixed to a K_d of 1 μM and undefined product binding equilibria were set to a K_d of 10 μM, with all association rate constants greater than 10⁸ M⁻¹s⁻¹ and all dissociation rate constants fixed at 1000 s⁻¹. The rate constants for activation and pyrimidine reduction were set initially to the values determined from the analytical fits applied in Figure 8A (1.0 s⁻¹ and 0.015 s⁻¹). As such convergence of the simulation and data is based only on variation of the binding constant for NADPH to the activated DPD•U•NADPH complex and the extinction coefficients associated with each phase. This simulation indicated that high affinity for NADPH in activated DPD•U•NADPH complex can account for the biphasic kinetics observed and predicts a subnanomolar dissociation constant for this ligand to this complex (annotated as *high affinity* in Figure 11).

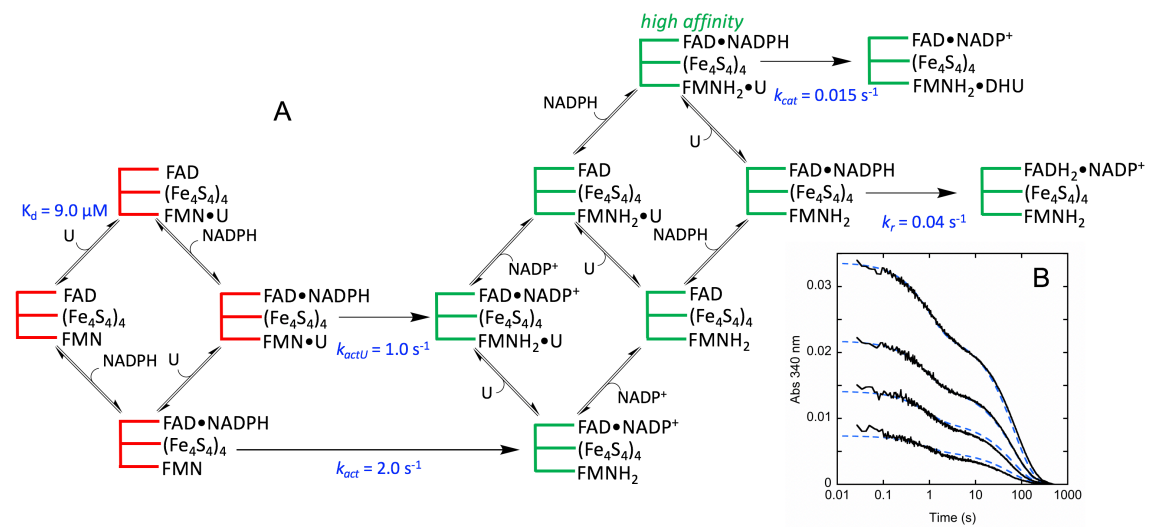


Figure 11. Kinetic model for DPD C671S that accounts for the 2:1 NADPH:pyrimidine stoichiometry observed in limiting NADPH single turnover experiments in the presence of uracil. A. The scheme depicts only activation and subsequent catalytic reduction of U by DPD C671S and is not inclusive of all ligand exchange equilibria. The activation and subsequent turnover of one subunit is shown using the notation of Gassner et al. (Biochemistry (1994) 33, 12184-12193). Activated forms of DPD are shown in green and inactive forms are shown in red. It is proposed that a parallel pathway for reductive activation of the enzyme exists in the absence of the pyrimidine substrate. Though the association of pyrimidine bridging the two pathways is depicted, no evidence for these equilibria is presented in this work. No reduced forms of Fe₂S₄ centers are shown, consistent with rapid electron transfer between active sites. B. Simulation of the biphasic kinetics shown in Figure 8A to the model shown in A. The data was modelled using enzyme and substrate concentrations shown shown for Figure 8A. With the exception of the dissociation constant for NADPH to the activated DPD•U•NADPH complex, undefined substrate binding equilibria were fixed to a K₀ of 1 μM and undefined product binding equilibria were set to a K₀ of 10 μM, with rapid ligand exchange rates (association rate constants > 108 M⁻¹s⁻¹ and dissociation rate constants fixed at 1000 s⁻¹). The rate constants for enzyme activation and pyrimidine reduction were fixed to the values determined from the analytical fits applied in Figure 8A (1.0 s⁻¹ and 0.015 s⁻¹). The k, step accounts for slow reduction of DPD in the absence of pyrimidine substrate, and is shown as reduction of the FAD, however, no evidence for the identity of the species reduced in this step is shown.

In the absence of other evidence, the model could imply a vestigial role for one of the two promoters in that only one is activated and subsequently reduces the pyrimidine, however, the second protomer presumably could be enlisted in subsequent turnovers and the single turnover approach used does not capture this process. The clearest evidence for this is that the turnover numbers in Table 1 correlate well with the rate constants measured for the second phase and were calculated by dividing by the DPD subunit concentration indicating both protomers are catalytic. Prior evidence indicative of alternating sites catalysis is available. In the structure of the closed state shown in Figure 10 (PDB ID 1GTH) the catalytic state of the two subunits in this DPD dimer differs. In one subunit the 5-iodo-substituent of the pyrimidine has been eliminated suggesting completion of catalysis, while in the other subunit has the iodo-group in place 7. Moreover, in 1998, Rosenbaum et al, observed biphasic reduction processes in the presence and absence of uracil under anaerobic conditions. In these experiments the amplitude of the initial

phase at 340 nm that reports NADPH consumption, equated to approximately one half the enzyme concentration ³⁰.

An alternative model posits cross dimer electron transfer and would require only reducing equivalents from pre-bound NADPH molecules. This model would rely on electron transfer to reduce the pyrimidine from the adjacent subunit's NADPH-FAD-iron-sulfur conduit and the closest approach for these centers is 24.5 Å, fully 15 Å further than the longest distance for proximal Fe₄S₄ centers that bridge the flavins in both subunits. It would therefore seem that the alternating subunit model is more likely.

Another consideration with regard to the design of the experiments depicted in Figures 5,7,8 & 9 is that limiting NADPH creates the possibility that the majority of the NADPH is bound. As such, the rate observed for the second phase in an alternating site model (reduction of the pyrimidine substrate) could be limited by the release rate constant for NADPH from the lagging subunit. However, the fact that the macroscopic rate constant, k_{cat} , for both enzyme forms reacting with both pyrimidine substrates agrees well with the rate constants measured for the second phase in transient state experiments (Table 1) and that these rates constants span four orders of magnitude, argues that the hydride transfer chemistry for the pyrimidine is predominantly rate limiting in catalysis.

Conclusive Remarks

The transient state single-turnover experiments shown here indicate that the reductive activation of DPD results in the reduction of one flavin per dimer consistent with alternating sites behavior. During the activation phase no evidence for reduced states of Fe₄S₄ centers is obtained.

Similarly, during the ensuing turnover phase only oxidation of NADPH and absorption changes attributed to pyrimidine substrate/product binding are observed even when the turnover is as slow as $0.00024 \, \text{s}^{-1}$. These both indicate that during pyrimidine reduction, electron transfer across the flavins and Fe₄S₄ centers is rapid relative to other process. If no intervening reduced state of the enzyme is observed, the net rate of transmission of electrons from NADPH to the pyrimidine (k_{cat}) must be determined exclusively by the rate of proton transfer from cysteine 671.

References

- [1] Lu, Z. H., Zhang, R., and Diasio, R. B. (1992) Purification and characterization of dihydropyrimidine dehydrogenase from human liver, *J Biol Chem 267*, 17102-17109.
- [2] Podschun, B., Jahnke, K., Schnackerz, K. D., and Cook, P. F. (1993) Acid base catalytic mechanism of the dihydropyrimidine dehydrogenase from pH studies, *J Biol Chem 268*, 3407-3413.
- [3] Podschun, B. (1992) Stereochemistry of NADPH oxidation by dihydropyrimidine dehydrogenase from pig liver, *Biochem Biophys Res Commun* 182, 609-616.
- [4] Schmitt, U., Jahnke, K., Rosenbaum, K., Cook, P. F., and Schnackerz, K. D. (1996) Purification and characterization of dihydropyrimidine dehydrogenase from Alcaligenes eutrophus, *Arch Biochem Biophys* 332, 175-182.
- [5] Podschun, B., Cook, P. F., and Schnackerz, K. D. (1990) Kinetic mechanism of dihydropyrimidine dehydrogenase from pig liver, J Biol Chem 265, 12966-12972.
- [6] Porter, D. J., Chestnut, W. G., Taylor, L. C., Merrill, B. M., and Spector, T. (1991) Inactivation of dihydropyrimidine dehydrogenase by 5-iodouracil, *J Biol Chem 266*, 19988-19994.
- [7] Dobritzsch, D., Ricagno, S., Schneider, G., Schnackerz, K. D., and Lindqvist, Y. (2002) Crystal structure of the productive ternary complex of dihydropyrimidine dehydrogenase with NADPH and 5-iodouracil. Implications for mechanism of inhibition and electron transfer, *J Biol Chem 277*, 13155-13166.
- [8] Heidelberger, C., Chaudhuri, N. K., Danneberg, P., Mooren, D., Griesbach, L., Duschinsky, R., Schnitzer, R. J., Pleven, E., and Scheiner, J. (1957) Fluorinated pyrimidines, a new class of tumour-inhibitory compounds, *Nature 179*, 663-666.

- [9] Rutman, R. J., Cantarow, A., Paschkis, E., and Allanoff, B. (1953) Studies on uracil utilization normal and acetaminofluorene-treated rats, *Science* 117, 282-283.
- [10] Rutman, R. J., Cantarow, A., and Paschkis, K. E. (1954) Studies in 2-acetylaminofluorene carcinogenesis. III. The utilization of uracil-2-C14 by preneoplastic rat liver and rat hepatoma, *Cancer Res 14*, 119-123.
- [11] Heidelberger, C. (1963) Biochemical Mechanisms of Action of Fluorinated Pyrimidines, *Exp Cell Res 24*, SUPPL9:462-471.
- [12] Kent, R. J., and Heidelberger, C. (1972) Fluorinated pyrimidines. XL. The reduction of 5fluorouridine 5'-diphosphate by ribonucleotide reductase, *Mol Pharmacol* 8, 465-475.
- [13] Reilly, R. T., Barbour, K. W., Dunlap, R. B., and Berger, F. G. (1995) Biphasic binding of 5-fluoro-2'-deoxyuridylate to human thymidylate synthase, *Mol Pharmacol* 48, 72-79.
- [14] Ludwiczak, J., Maj, P., Wilk, P., Fraczyk, T., Ruman, T., Kierdaszuk, B., Jarmula, A., and Rode, W. (2016) Phosphorylation of thymidylate synthase affects slow-binding inhibition by 5-fluoro-dUMP and N(4)-hydroxy-dCMP, *Mol Biosyst 12*, 1333-1341.
- [15] Longley, D. B., Harkin, D. P., and Johnston, P. G. (2003) 5-fluorouracil: mechanisms of action and clinical strategies, *Nat Rev Cancer 3*, 330-338.
- [16] Milano, G., and Etienne, M. C. (1994) Dihydropyrimidine dehydrogenase (DPD) and clinical pharmacology of 5-fluorouracil (review), *Anticancer Res 14*, 2295-2297.
- [17] Heggie, G. D., Sommadossi, J. P., Cross, D. S., Huster, W. J., and Diasio, R. B. (1987) Clinical pharmacokinetics of 5-fluorouracil and its metabolites in plasma, urine, and bile, *Cancer Res* 47, 2203-2206.

- [18] de Bono, J. S., and Twelves, C. J. (2001) The oral fluorinated pyrimidines, *Invest New Drugs* 19, 41-59.
- [19] Porter, D. J., Chestnut, W. G., Merrill, B. M., and Spector, T. (1992) Mechanism-based inactivation of dihydropyrimidine dehydrogenase by 5-ethynyluracil, *J Biol Chem 267*, 5236-5242.
- [20] Baccanari, D. P., Davis, S. T., Knick, V. C., and Spector, T. (1993) 5-Ethynyluracil (776C85): a potent modulator of the pharmacokinetics and antitumor efficacy of 5-fluorouracil, *Proc Natl Acad Sci U S A 90*, 11064-11068.
- [21] Spector, T., Harrington, J. A., and Porter, D. J. (1993) 5-Ethynyluracil (776C85): inactivation of dihydropyrimidine dehydrogenase in vivo, *Biochem Pharmacol* 46, 2243-2248.
- [22] Porter, D. J., Harrington, J. A., Almond, M. R., Lowen, G. T., Zimmerman, T. P., and Spector, T. (1994) 5-ethynyl-2(1H)-pyrimidinone: aldehyde oxidase-activation to 5-ethynyluracil, a mechanism-based inactivator of dihydropyrimidine dehydrogenase, *Biochem Pharmacol* 47, 1165-1171.
- [23] Schnackerz, K. D., Dobritzsch, D., Lindqvist, Y., and Cook, P. F. (2004) Dihydropyrimidine dehydrogenase: a flavoprotein with four iron-sulfur clusters, *Biochim Biophys Acta 1701*, 61-74.
- [24] Fagan, R. L., Jensen, K. F., Bjornberg, O., and Palfey, B. A. (2007) Mechanism of flavin reduction in the class 1A dihydroorotate dehydrogenase from Lactococcus lactis, *Biochemistry 46*, 4028-4036.
- [25] Reis, R. A. G., Calil, F. A., Feliciano, P. R., Pinheiro, M. P., and Nonato, M. C. (2017) The dihydroorotate dehydrogenases: Past and present, *Arch Biochem Biophys* 632, 175-191.

- [26] Stott, K., Saito, K., Thiele, D. J., and Massey, V. (1993) Old Yellow Enzyme. The discovery of multiple isozymes and a family of related proteins, *J Biol Chem 268*, 6097-6106.
- [27] Dobritzsch, D., Schneider, G., Schnackerz, K. D., and Lindqvist, Y. (2001) Crystal structure of dihydropyrimidine dehydrogenase, a major determinant of the pharmacokinetics of the anti-cancer drug 5-fluorouracil, *EMBO J 20*, 650-660.
- [28] Podschun, B., Wahler, G., and Schnackerz, K. D. (1989) Purification and characterization of dihydropyrimidine dehydrogenase from pig liver, *Eur J Biochem 185*, 219-224.
- [29] Rosenbaum, K., Schaffrath, B., Hagen, W. R., Jahnke, K., Gonzalez, F. J., Cook, P. F., and Schnackerz, K. D. (1997) Purification, characterization, and kinetics of porcine recombinant dihydropyrimidine dehydrogenase, *Protein Expr Purif* 10, 185-191.
- [30] Rosenbaum, K., Jahnke, K., Curti, B., Hagen, W. R., Schnackerz, K. D., and Vanoni, M. A. (1998) Porcine recombinant dihydropyrimidine dehydrogenase: comparison of the spectroscopic and catalytic properties of the wild-type and C671A mutant enzymes, *Biochemistry 37*, 17598-17609.
- [31] Porter, D. J., and Spector, T. (1993) Dihydropyrimidine dehydrogenase. Kinetic mechanism for reduction of uracil by NADPH, *J Biol Chem 268*, 19321-19327.
- [32] Shiotani, T., and Weber, G. (1981) Purification and properties of dihydrothymine dehydrogenase from rat liver, *J Biol Chem 256*, 219-224.
- [33] Rosenbaum, K., Jahnke, K., Schnackerz, K. D., and Cook, P. F. (1998) Secondary tritium and solvent deuterium isotope effects as a probe of the reaction catalyzed by porcine recombinant dihydropyrimidine dehydrogenase, *Biochemistry 37*, 9156-9159.

- [34] Lohkamp, B., Voevodskaya, N., Lindqvist, Y., and Dobritzsch, D. (2010) Insights into the mechanism of dihydropyrimidine dehydrogenase from site-directed mutagenesis targeting the active site loop and redox cofactor coordination, *Biochim Biophys Acta* 1804, 2198-2206.
- [35] Porter, D. J. (1994) Dehalogenating and NADPH-modifying activities of dihydropyrimidine dehydrogenase, *J Biol Chem 269*, 24177-24182.
- [36] Beaupre, B. A., Roman, J. V., and Moran, G. R. (2020) An improved method for the expression and purification of porcine dihydropyrimidine dehydrogenase, *Protein Expr Purif* 171, 105610.
- [37] Moran, G. R. (2019) Anaerobic methods for the transient-state study of flavoproteins: The use of specialized glassware to define the concentration of dioxygen, *Methods Enzymol* 620, 27-49.
- [38] Krakow, G., and Vennesland, B. (1961) The equilibrium constant of the dihydroorotic dehydrogenase reaction, *J Biol Chem 236*, 142-144.
- [39] Rowland, P., Björnberg, O., Nielsen, F. S., Jensen, K. F., and Larsen, S. (1998) The crystal structure of Lactococcus lactis dihydroorotate dehydrogenase A complexed with the enzyme reaction product throws light on its enzymatic function, *Prot.Sci.* 7, 1269-1279.

Acknowledgements

This research was supported by Loyola University College of Arts and Sciences and National Science Foundation Grant 1904480 to G.R.M.

Uniprot Identifiers

Sus Scrofa DPD - Q28943

TOC

